

# Nucleosome shape dictates chromatin-fiber structure

Martin Depken,<sup>1,2,3\*</sup> Helmut Schiessel<sup>3</sup>

<sup>1</sup> Max Planck Institute for the Physics Complex Systems,  
Nöthnitzer Straße 38, 01187 Dresden, Germany

<sup>2</sup>Max-Planck Institute for Molecular Cell Biology and Genetics,  
Pfotenhauerstr. 108, 01307 Dresden, Germany

<sup>3</sup>Instituut-Lorentz for Theoretical Physics, Universiteit Leiden,  
Postbus 9506, 2300 RA Leiden, The Netherlands

\*To whom correspondence should be addressed; E-mail: depken@pks.mpg.de.

**Apart from being the gateway for all access to the eukaryotic genome, chromatin has in recent years been identified as carrying an epigenetic code regulating transcriptional activity. The detailed knowledge of this code contrasts the ignorance of the fiber structure which it regulates, and none of the suggested fiber models are capable of predicting the most basic quantities of the fiber (diameter, nucleosome line density, etc.). We address this three-decade-old problem by constructing a simple geometrical model based on the nucleosome shape alone. Without fit parameters we predict the observed properties of the condensed chromatin fiber (e.g. its 30 nm diameter), the structure, and how the fiber changes with varying nucleosome repeat length. Our approach further puts the plethora of previously suggested models within a coherent framework, and opens the door to detailed studies of the interplay between chromatin structure and function.**

Eukaryotic DNA is wrapped around histone proteins, resulting in a string of wedge-shaped nucleosomes connected via short stretches of linker DNA. Under physiological salt concentrations this string can undergo additional folding, forming what is referred to as the 30 nm fiber. Whereas the structure of the nucleosome is known to atomic resolution (1), the three-dimensional arrangement of nucleosomes in the 30 nm fiber remains poorly understood — despite three decades of experiments and model building (2). The wide range of models documented in the literature can be divided into roughly two classes: the traditional solenoid models (3) and the crossed linker models (4). Unfortunately, neither type provide criteria to identify the optimal fiber geometry, and basic quantities like the fiber diameter are ultimately fixed by the fine tuning of unknown parameters. This lack of predictive power and the fact that many

experiments (5, 6, 7, 8, 9) were likely performed on amorphous samples (10) are arguably the main reasons why the structure has remained unresolved for so long. Some of the experimental issues have recently been overcome through the reconstitution of highly regular fibers (11, 12), but a comprehensive modeling effort determining the structure is still lacking. We take inspiration from previous success of geometric arguments when applied to information-carrying structures (13) and address this problem by considering all fibers satisfying the geometric condition that the nucleosome core particles (NCPs) pack densely on the periphery of the fiber (2) (see Fig. 1 a). Without free parameters this enables us to make definite predictions that are all born out when compared to the new regular reconstituted fibers (11, 12). Our approach makes the implicit assumption the short range attraction between NCPs (14, 15, 16) constitute the dominant mode of interaction in dense chromatin fibers, being only weakly modulated by the soft contribution from the DNA-linker backbone. Taking this view, the problem of determining the structure of the chromatin fiber splits into two parts: the identification of dense configurations of NCPs on the periphery of the fiber, and the estimation of the energetic contribution from the linker backbone in order to determine which structure is realized.

First addressing the formation of a dense shell we note that NCPs aggregate into arcs in solution (17), indicating that their wedge-shaped form (1) can play a key role in dictating large scale arrangements of interacting nucleosomes. Drawing on this, we take the *effective shape* of the NCP as being that of a wedge shaped cylinder (see Fig. 1 b). In Figure 1 c we show how a dense packing of nucleosome footprints on a periodic strip is a necessary condition for a dense three-dimensional packing of nucleosomes in the fiber. By assuming a dense packing the footprints are forced into helical ribbons winding along the fiber. These are formed along either of the footprints symmetry axes. Models normally referred to as interdigitated (11, 18) belong to the set of dense packings where the ribbons form along the major axis (NCPs stacking side to side). Here we assume the NCPs to stack face to face, corresponding to footprints forming ribbons along their minor axis (see Supplementary note for the modifications to the below in the case of interdigitated structures). Such stackings of NCPs aggregate spontaneously under the right solvent conditions (17, 19), and is also what best utilizes any short range attractive interaction. For a dense footprint packing, the nucleosome line density (NLD)  $\sigma$  is simply the width of the strip onto which they pack, divided by the foot print area,

$$\sigma = \frac{\pi(D - a)}{ab}. \quad (1)$$

The manner in which the ribbons spiral up along the fiber, parameterized by the ribbon angle  $\gamma$ , is set by the requirement that the  $N_{\text{rib}}$  ribbons precisely fill up the periodic strip (see Fig. 1 c),

$$N_{\text{rib}} \frac{a}{\cos \gamma} = \pi(D - a). \quad (2)$$

In addition we require that the backbone connects all the nucleosomes in a regular fashion. Denote by  $N_{\text{step}}$  the distance across ribbons between connected nucleosomes (see Fig. 1 a). The necessary and sufficient condition for a regular backbone winding (BW) — completely defined

by the pair  $(N_{\text{rib}}, N_{\text{step}})$  — is the existence of two integers  $n$  and  $k$  with  $0 \leq n \leq k \leq N_{\text{rib}}$  such that

$$kN_{\text{step}} - nN_{\text{rib}} = 1. \quad (3)$$

Equation 3 ensures that neighboring ribbons are eventually connected (after  $k$  steps and  $n$  turns, see Supplementary note) and hence all ribbons are visited by the backbone (c.f. (4, 2), which only connects half of the NCPs). The trivial BW  $(N_{\text{rib}}, 1)$  corresponds to the backbone connecting nucleosomes in neighboring ribbons (since  $N_{\text{step}} = 1$ , see Fig. 1 a). Such a backbone can be found for fibers with any number of ribbons since with  $n = 0$  and  $k = 1$  condition Equation 3 is always satisfied. The classical solenoid model (3) has a (1, 1) BW, and all the models considered by Wong *et al.* (20) have trivial BWs. By scanning through the finite number of possible  $n$ 's and  $k$ 's one finds all additional non-trivial BWs, extending the set of crossed-linker models to (5, 2), (7, 2), (7, 3), (8, 3), and so on. Thus this approach exhaustively covers all major contending models for the fiber structure (3, 7, 21, 6, 4, 2) (solenoid models, crossed linker models, interdigitated models, etc.), including some specific models not previously considered, and puts them firmly within a coherent framework.

Returning to the full three-dimensional packing of nucleosomes we note that all admissible footprint packings correspond to NCPs packed together with different *effective* wedge angles (see Fig. 1 b). Through considering the curvature along the ribbons it is straightforward to relate the effective wedge angle to the fiber diameter (see Supplementary note). Within the relevant parameter ranges the exact expression can be approximated as

$$\alpha \approx \frac{2b}{D - a} \left( 1 - \left[ \frac{aN_{\text{rib}}}{\pi(D - a)} \right]^2 \right), \quad (4)$$

with an accuracy of a couple of tenths of a degree. For any specific fiber diameter  $D$  and number of ribbons  $N_{\text{rib}}$  this directly gives the effective wedge angle, and it can easily be inverted to give the possible fiber diameters for any specific effective wedge angle. In Figure 2 a we show how the effective wedge angle varies with fiber diameter for fibers with up to ten ribbons. In what follows we will use the effective NCP diameter  $a = 11.5$  nm and average height  $b = 6.0$  nm as deduced for the close packings of NCPs into columnar quasi-hexagonal crystals (19) under physiological salt concentrations and moderate pressures. We are ultimately interested in the *in vivo* situation where there are additional linker histones present, bringing the in and out going DNA at each nucleosome into a stem structure (22) (see Fig. 1 b). Taking this into account, we require  $D > 2(l_{\text{stem}} + a)$  in order to avoid steric interactions between stems on opposite sides of the fiber. Here  $l_{\text{stem}} = 3$  nm is the length of the induced stem as measured by Bednar *et al.* (22). In Figure 2 b we illustrate all fibers and BWs with a diameter of 33 nm. They include the solenoid model (1, 1) (3), the two-start helix (2, 1) (12) and the crossed linker model (5, 2) (4). It is clear from the number of possible structures that fixing the fiber diameter tells us little about the internal structure of the fiber, though it explains the wide range of models suggested in the literature; all made consistent with the experimental findings but with little predictive power. Instead we take a reductionist approach and enforce the microscopic

condition of optimal dense face-to-face stacking of nucleosomes. In experiments by Dubochet and Noll (17) unconstrained nucleosomal arcs were observed with the effective wedge angle  $\alpha = 8^\circ$  for the NCP repeat unit. This will be the effective wedge angle assumed throughout the rest of this paper. With this microscopic condition we directly get a discrete set of possible shell structures, three of which are shown in Figure 2 c (structures A, B, and C), and all of which are clearly distinguished from each other on the level of the fiber diameter and NLD (see Table 1). Here we do not discuss the very wide fibers, one of which is displayed in the inset of Figure 2 a. These structures might never be realized in chromatin, but are similar to the gigantic tubes of NCPs observed by Dubochet and Noll (17). The results of the simple assumption of a dense packing of nucleosomal wedges are summarized in Table 1, where we list all fibers with a fiber diameter up to 63 nm. As detailed below some of these have already been observed, while others might still be found through further experiments.

Armed with a small set of possible shell structures, we now examine the linker backbone to determine which of these is realized for any specific nucleosomal repeat length. Though we lack a precise model for the energetics of the backbone, we can still put upper and lower bounds on the possible linker lengths for a specific shell structure and BW. The lower bound is set by the shortest distance between two successive stems along the backbone. This depends not only on the BW  $(N_{\text{rib}}, N_{\text{step}})$  but also on the relative helicity of backbone and ribbons. We denote structures where ribbons and backbone have the same helicity by  $(N_{\text{rib}}, N_{\text{step}})^+$ , and by  $(N_{\text{rib}}, N_{\text{step}})^-$  in the opposite case. The upper limit for the linker length is set by the excluded volume constraint on the inside of the fiber. We assume that due to the presence of cationic histone tails the highly charged linker DNA can be hexagonally packed with a shortest centre-to-centre distance set by the DNA diameter  $d_{\text{DNA}} = 2$  nm. The resulting limits on the linker lengths are indicated in Table 1. We thus see that for the shortest repeat lengths the realized structure must always be  $(5, 1)^\pm$  or  $(5, 2)^\pm$ . These feature a 33 nm diameter, from which the 30 nm fiber derives its name. Of these two structures we expect  $(5, 2)^\pm$  to be realized since it allows for the straightest linkers (see Fig. 2 c, structure A). When increasing the linker length the fiber must take on another structure before the maximum repeat length of 210 bp. The fact that  $(7, 3)^\pm$  (possible for repeat lengths over 207 bp) has the straightest linkers (see Fig. 2 c, structure C) makes it a good candidate for the target structure. Thus, through the very simple, geometric, and microscopic condition of an optimal nucleosome packing combined with rudimentary arguments concerning the backbone, we are able to make predictions concerning the precise structure realized for different nucleosomal repeat lengths.

Having discussed the theoretically possible fibers for different repeat lengths, and identified a plausible transition point between structures, we now compare this with recent results on dense reconstituted fibers. Robinson *et al.* (11) observed that such fibers clustered into two sets, each signified by a specific fiber diameter and NLD (see Fig. 3). As pointed out by Wong *et al.* (20), a similar clustering is also seen for the native fibers examined by Williams *et al.* (6). Since the fiber diameter and the NLD are linearly related through condition Equation 1, we can use this as a direct test of our approach. In Figure 3 we plot this relation together with the observed fiber diameter and nucleosome line densities (11). Our model is consistent with the experimental data

and manages to account for both thin and thick fibers without any fit parameters. In Figure 2 we have indicated the average diameters of the two clusters observed by Robinson *et al.* (11). The structures predicted by our model (Fig. 2 a and c, structures A and C) are the only fibers within the error bars of the experiments. It can also be seen that these predictions are rather robust against changes in the effective wedge angle. In addition, the transition between fiber structures is observed somewhere between repeat lengths of 207 and 217 bp, which is also captured by our model. Apparently contradicting these results is another recent set of experiments (12) suggesting a two-ribbon structure. These were performed on short fibers (10-12 nucleosomes), and would thus be unlikely to capture the structures suggested here (5 and 7 ribbons) since they only allow for around two nucleosomes to stack in each ribbon. In line with the basic assumption of our model, that nucleosome interactions drive the assembly of the fiber, we expect short fibers to favor fewer ribbons in order to minimize the number of nucleosome faces exposed to the solution. The same reasoning applies to inferring the arrangement of nucleosomes in the fiber from the crystallographic structure of the tetra-nucleosome (23). Thus we conclude that our zero-fit-parameter model is consistent with all experimental findings on regular fibers to date.

Our model could be further tested through e.g. linear dichroism (8, 9) studies determining the ribbon angle  $\gamma$  for these newly available structures. It would also be interesting to see if structures like  $(8, 3)^\pm$  or  $(9, 4)^\pm$  are ever realized for repeat lengths longer than those investigated by Robinson *et al.* (11). Moving away from the 10 bp ladder (set by DNA's helical repeat length) used by Robinson *et al.* would further elucidate whether it is the bend or twist energy of the linker DNA that dictates the chosen structures. Our model also suggests that the predicted structures are insensitive to a certain amount of variations in the nucleosome repeat length. With the inclusion of an energetic model for the linker backbone the above development should form the basis for statistical and kinetic studies of how *in vivo* variations and correlation in repeat length (24) affect the locally realized structure, its stability, and thus the observed condensation-decondensation transition of the 30 nm fiber. *In vitro*, this transition can be probed by a change of ionic conditions (22), or the application of a sufficiently large external force, e.g. in a single-molecule-experiment using optical tweezers (25). *In vivo*, this can be done by the acetylation of histone tails (26, 27), thus offering a straightforward way of increasing the accessibility to the packed genetic material. Understanding the structure of the fiber now opens the door to detailed study of this transition, and its connection to the histone code (28, 29, 27). Ultimately this structural knowledge should be combined with biochemical studies in order to move towards a comprehensive understanding of the subtle interplay between structure and function in chromatin (30).

## Acknowledgments

We would like to acknowledge fruitful discussions with Ralf Everaers, Nima Hamedani Radja, Marc Emanuel, and John van Noort. We thank Eric Galburt, Stephan Grill, and Mirjam Mayer for comments on the manuscript. A special thank is owed Wim van Saarloos without whom this

research would not have been possible. M.D. acknowledges support from the physics foundation FOM.

## References and Notes

1. K. Luger, A. W. Mäder, R. K. Richmond, D. F. Sargent, T. J. Richmond, *Nature* **389**, 251 (1997).
2. K. van Holde, J. Zlatanova, *Semin Cell Dev Biol* p. in press (2007).
3. J. T. Finch, A. Klug, *Proc Natl Acad Sci U S A* **73**, 1897 (1976).
4. C. L. Woodcock, S. A. Grigoryev, R. A. Horowitz, N. Whitaker, *Proc Natl Acad Sci U S A* **90**, 9021 (1993).
5. J. Widom, J. T. Finch, J. O. Thomas, *EMBO J* **4**, 3189 (1985).
6. S. P. Williams, *et al.*, *Biophys J* **49**, 233 (1986).
7. A. Worcel, S. Strogatz, D. Riley, *Proc Natl Acad Sci U S A* **78**, 1461 (1981).
8. J. D. McGhee, J. M. Nickol, G. Felsenfeld, D. C. Rau, *Cell* **33**, 831 (1983).
9. D. Sen, S. Mitra, D. M. Crothers, *Biochemistry* **25**, 3441 (1986).
10. K. van Holde, J. Zlatanova, *J Biol Chem* **270**, 8373 (1995).
11. P. J. J. Robinson, L. Fairall, V. A. T. Huynh, D. Rhodes, *Proc Natl Acad Sci U S A* **103**, 6506 (2006).
12. B. Dorigo, *et al.*, *Science* **306**, 1571 (2004).
13. J. D. Watson, F. H. Crick, *Nature* **171**, 737 (1953).
14. S. Mangelot, A. Leforestier, P. Vachette, D. Durand, F. Livolant, *Biophys J* **82**, 345 (2002).
15. S. Mangelot, *The European Physical Journal E-Soft Matter* **7**, 221 (2002).
16. F. Mühlbacher, H. Schiessel, C. Holm, *Phys Rev E Stat Nonlin Soft Matter Phys* **74**, 031919 (2006).
17. J. Dubochet, M. Noll, *Science* **202**, 280 (1978).
18. P. J. J. Robinson, D. Rhodes, *Curr Opin Struct Biol* **16**, 336 (2006).
19. S. Mangelot, A. Leforestier, D. Durand, F. Livolant, *J Mol Biol* **333**, 907 (2003).

20. H. Wong, J.-M. Victor, J. Mozziconacci, *PLoS ONE* **2**, e877 (2007).
21. V. Makarov, S. Dimitrov, V. Smirnov, I. Pashev, *FEBS Lett* **181**, 357 (1985).
22. J. Bednar, *et al.*, *Proc Natl Acad Sci U S A* **95**, 14173 (1998).
23. T. Schalch, S. Duda, D. F. Sargent, T. J. Richmond, *Nature* **436**, 138 (2005).
24. E. Segal, *et al.*, *Nature* **442**, 772 (2006).
25. Y. Cui, C. Bustamante, *Proc Natl Acad Sci U S A* **97**, 127 (2000).
26. P. J. Horn, C. L. Peterson, *Science* **297**, 1824 (2002).
27. M. F. Dion, S. J. Altschuler, L. F. Wu, O. J. Rando, *Proc Natl Acad Sci U S A* **102**, 5501 (2005).
28. B. D. Strahl, C. D. Allis, *Nature* **403**, 41 (2000).
29. T. Jenuwein, C. D. Allis, *Science* **293**, 1074 (2001).
30. R. D. Kornberg, Y. Lorch, *Nat Struct Mol Biol* **14**, 986 (2007).

Table 1: The predicted fiber structures. The table displays all the calculated properties of the fibers consistent with the structure of the nucleosome. They are (left to right): fiber structure, fiber diameter, nucleosome line density, angle formed between ribbons and fiber axis, minimum nucleosomal repeat length, and maximum nucleosomal repeat length. The minimum repeat length differs for different relative helicities between linker backbone and ribbons, the value for opposite relative helicity being indicated within parenthesis (for the case of at least one bp difference between the two). Empty fields take the values of fields directly above.

Structure	$D(\text{nm})$	$\sigma(1/\text{nm})$	$ \gamma (\text{deg})$	$l_{\text{repeat}}(\text{bp}) >$	$l_{\text{repeat}}(\text{bp}) <$
$(5, 1)^\pm$	33	1.0	29	172(171)	210
$(5, 2)^\pm$				175	
$(6, 1)^\pm$	38	1.2	33	178(177)	269
$(7, 1)^\pm$	44	1.5	38	184(183)	343
$(7, 2)^\pm$				199(198)	
$(7, 3)^\pm$				207	
$(8, 1)^\pm$	52	1.8	42	190(189)	440
$(8, 3)^\pm$				225	
$(9, 1)^+$	63	2.4	50	200(198)	605
$(9, 2)^+$				230(229)	
$(9, 4)^\pm$				264	

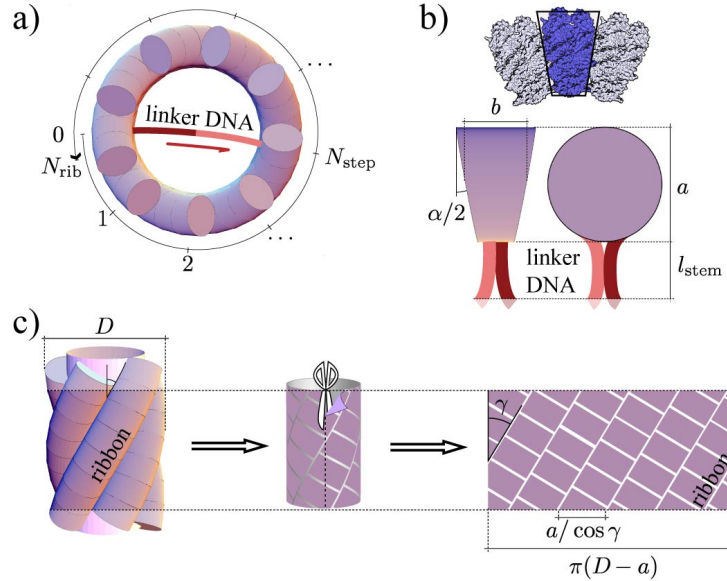


Figure 1: The model of the dense chromatin fiber. **a)** In a dense chromatin fiber the nucleosomes pack on the outside of the fiber, and the linkers are situated on the inside. Here the ( $N_{\text{rib}} = 9, N_{\text{step}} = 4$ ) backbone is illustrated, completely specifying the way the nucleosomes are connected. **b)** Illustration of how three nucleosomes stack, and how this relates to the *effective* wedge shape of the nucleosome (outlined). By using the term effective wedge shape we stress that the nucleosome itself need not form a perfect wedge, but rather that we rely on the experimental observation (17) that when they aggregate one can identify a wedge shaped repeat unit. Onto the wedge shaped cylinder we attach a rigid stem (22) to represent the in and out going DNA and a linker histone (not shown). **c)** Illustration of how a dense nucleosome-footprint packing on a cylinder running through the nucleosome centers is a necessary condition for a dense three-dimensional structure. Also indicated are the ribbons induced by the dense packing, together with the angle  $\gamma$  they make with the fiber axis.

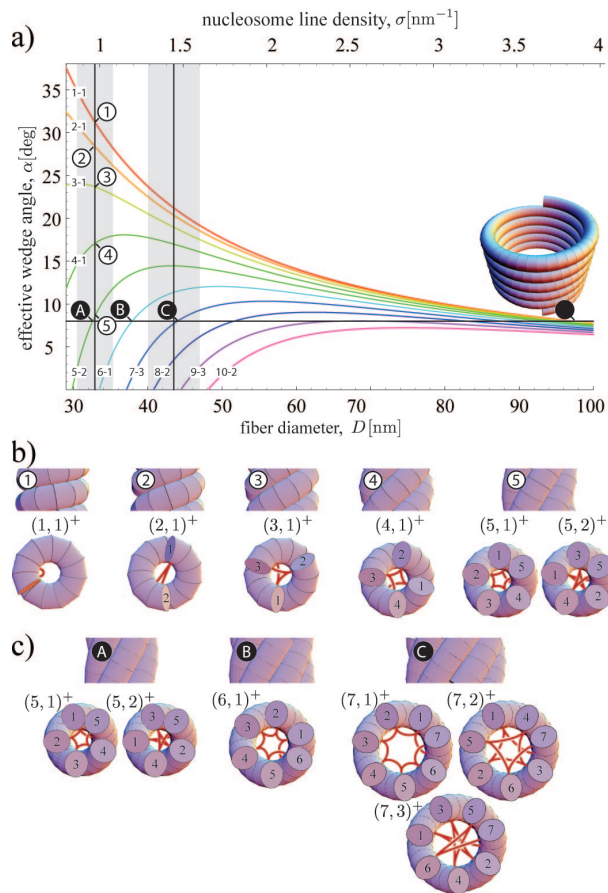


Figure 2: The predicted fibers. **a)** Plot of how the effective wedge angle  $\alpha$  varies with fiber diameter  $D$  (or, equivalently nucleosome line density  $\sigma$ ) for fibers with up to ten ribbons. Each curve is labeled as: number of ribbons - number of possible backbones. Indicated is also the effective wedge angle measured by Dubochet and Noll (17) and used in this paper to predict the fiber structures. A giant fiber solution with 87 nm diameter, and similar to the ones seen by Dubochet and Noll (17), is displayed in the inset. Further indicated are the average fiber diameters for the two different sets of fibers observed by Robinson *et al.* (11) (see also Fig. 3), with the area including one standard deviation indicated in grey. **b)** All solutions with different effective wedge angles achieved by fixing the fiber diameter to 33 nm (point 1-5 in Panel a), together with the available backbones. **c)** Some of the structures predicted by fixing the effective wedge angle to the value measured by Dubochet and Noll (17) (points A-C in Panel a), together with the allowed backbones. The fibers with 5 (A) and 7 (C) ribbons come very close to the structures observed by Robinson *et al.* (11) for dense reconstituted fibers.

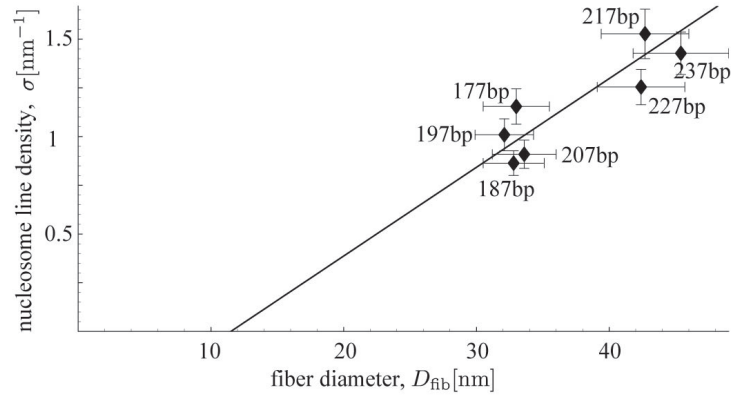


Figure 3: Experimental observations on dense fibers. Re-representation of data published by Robinson *et al.* (11) for reconstituted fibers with different nucleosomal repeat lengths (indicated). The data points are seen to cluster around two specific diameters,  $D = 33$  nm and 44 nm, and nucleosome line densities,  $\sigma = 1.0 \text{ nm}^{-1}$  and  $1.4 \text{ nm}^{-1}$ . The error bars indicate one standard deviation. Also shown is the linear relation between fiber diameter and nucleosome line density predicted by our model Eq. 1. It is seen to be consistent with both thin and thick fibers, without any adjustable parameters.

## Supporting Notes

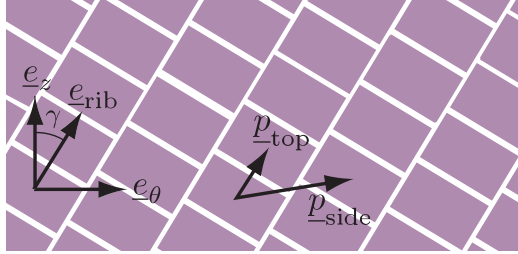


Figure S1: Footprint packing structure. The footprint packing defined in Figure 1 c of the main text, with lattice vectors  $\underline{p}_{\text{top}}$  and  $\underline{p}_{\text{side}}$  indicated, together with the unit vectors  $\underline{e}_z$ ,  $\underline{e}_r$ , and  $\underline{e}_{\text{rib}}$ .

**The relation defining the backbone winding:** Building on the footprint packings displayed in Figure 1 of the main text, define the vector  $\underline{p}_{\text{top}}$  as the vector connecting the nucleosome at its base (see Fig. S1) with the next nucleosome placed in the same ribbon which is encountered when moving along the backbone. In a similar manner define  $\underline{p}_{\text{side}}$  as ending at the next nucleosome encountered in the ribbon neighboring to the right. Let  $k_{\text{top}}$  be the number of steps taken along the backbone when going between the nucleosomes connected by  $\underline{p}_{\text{top}}$ , and  $n_{\text{top}}$  the number of times the fiber was circled in doing so. Define  $k_{\text{side}}$  and  $n_{\text{side}}$  in the analogous manner. Then we have

$$\underline{p}_{\text{top}} = (k_{\text{top}}\Delta - \pi(D - a)n_{\text{top}})\underline{e}_{\theta} + \frac{k_{\text{top}}}{\sigma}\underline{e}_z,$$

$$\underline{p}_{\text{side}} = (k_{\text{top}}\Delta - \pi(D - a)n_{\text{side}})\underline{e}_{\theta} + \frac{k_{\text{side}}}{\sigma}\underline{e}_z,$$

where  $\sigma$  is the nucleosome line density along the fiber, and  $\Delta$  is the circumferential distance between nucleosomes following each other along the backbone. For the packing of ribbons to be dense, the parallelogram spanned by these two vectors must be of the same area as the footprint,

$$ab = \underline{p}_{\text{side}} \wedge \underline{p}_{\text{top}} = \pi(D - a)(n_{\text{top}}k_{\text{side}} - n_{\text{side}}k_{\text{top}})/\sigma.$$

Using Equation 1 of the main text this becomes

$$n_{\text{top}}k_{\text{side}} - n_{\text{side}}k_{\text{top}} = 1.$$

Before returning to the same ribbon, all ribbons traversed on the outside of the fiber in the first step has to be visited exactly once (ribbon 1, 2,  $\dots$ ,  $N_{\text{step}} - 1$  of Fig. 1 a of the main text). This can only be done during successive turns around the fiber, and thus  $N_{\text{step}} = n_{\text{top}}$ . Also, before returning to the same ribbon, all other ribbons must have been visited exactly once, giving  $k_{\text{top}} = N_{\text{rib}}$ , where  $N_{\text{rib}}$  is the number of ribbons in the fiber. Thus Equation 3 of the main text follows.

**Approximate relationship for wedge angle:** The curvature tensor for the cylinder surface defined in Figure 1 a of the main text is given in the orthonormal basis  $(\underline{e}_\theta, \underline{e}_z)$  (see Fig. S1) as

$$\mathbf{K} = \begin{pmatrix} 2/(D-a) & 0 \\ 0 & 0 \end{pmatrix},$$

and the unit vector aligned with the ribbons is given by

$$\underline{e}_{\text{rib}} = \sin \gamma \underline{e}_\theta + \cos \gamma \underline{e}_z.$$

With this we can calculate the radius of curvature along the ribbons,  $R_{\text{rib}}$ , as

$$1/R_{\text{rib}} = \underline{e}_{\text{rib}} \cdot \mathbf{K} \cdot \underline{e}_{\text{rib}} = \frac{2 \sin^2 \gamma}{D-a}.$$

The wedge angle is now approximated by

$$\alpha \approx b/R_{\text{rib}} = \frac{2b \sin^2 \gamma}{D-a},$$

which by use of Equation 2 in the main text directly gives Equation 4 of the main text.

**Modifications for interdigitated models:** For the interdigitated models Equation 1 and Equation 3 stay the same, while Equation 2, and Equation 4 become

$$N_{\text{rib}} \frac{b}{\cos \gamma} = \pi(D-a)$$

and

$$\alpha \approx 2\pi N_{\text{rib}}^2 \left( \frac{b}{\pi(D-a)} \right)^3$$

respectively.